


## Article

# Periodicity of Superatomic Hybrid Orbitals in Substituted Superatoms and Superatomic-like $X@Ga_{12}$ ( $X = Li \sim Kr$ ) Clusters

Takaki Nishimura <sup>1</sup> , Teruyuki Toba <sup>1</sup>, Genta Sakane <sup>2</sup> and Tomohiko Ishii <sup>1,\*</sup>
<sup>1</sup> Department of Advanced Materials Science, Graduated School of Engineering, Kagawa University, Takamatsu 761-0396, Japan; s20d552@stu.kagawa-u.ac.jp (T.N.); s18g576@gmail.com (T.T.)

<sup>2</sup> Natural Sciences Section, Center for Fundamental Education, Institute for the Advancement of Higher Education, Okayama University of Science, Okayama 700-0005, Japan; gsakane@chem.ous.ac.jp

\* Correspondence: ishii.tomohiko@kagawa-u.ac.jp; Tel.: +81-87-864-2414

**Abstract:** A superatom is a cluster composed of a specific number of atoms. We recently found that the superatom-like  $X@Ga_{12}$  ( $X = Li \sim Kr$ ) clusters has the periodic energy levels of the specific orbitals 2S and 2P by means of the DV- $X\alpha$  molecular orbital calculation method. This periodicity in energy levels has not been seen in 1D or 1F orbitals. We supposed that the periodicity of the energy levels of the 2S and 2P superatomic-like orbitals come from the same symmetry between atomic orbitals as the central atom X and the surrounding specific orbitals, according to the Jellium model. Both the s and p atomic orbitals of the central atom X in the superatom-like  $X@Ga_{12}$  have a large shielding effect, suggesting that the s and p atomic orbitals interact strongly with both 2S and 2P superatomic-like orbitals. The energy level periodicity has the potential to periodically change the number of electrons located in the 1D and 1F orbitals, which is related to magnetic properties and is expected to be useful for novel magnetic devices by periodically controlling the magnetism of superatoms.

**Keywords:** molecular orbital; orbital periodicity in the superatom; DV- $X\alpha$  method; superatomic orbital; superatomic-like orbital



**Citation:** Nishimura, T.; Toba, T.; Sakane, G.; Ishii, T. Periodicity of Superatomic Hybrid Orbitals in Substituted Superatoms and Superatomic-like  $X@Ga_{12}$  ( $X = Li \sim Kr$ ) Clusters. *Crystals* **2022**, *12*, 543. <https://doi.org/10.3390/cryst12040543>

Academic Editors: Paolo Restuccia and James Ren

Received: 22 February 2022

Accepted: 8 April 2022

Published: 12 April 2022

**Publisher's Note:** MDPI stays neutral with regard to jurisdictional claims in published maps and institutional affiliations.



**Copyright:** © 2022 by the authors. Licensee MDPI, Basel, Switzerland. This article is an open access article distributed under the terms and conditions of the Creative Commons Attribution (CC BY) license (<https://creativecommons.org/licenses/by/4.0/>).

## 1. Introduction

A superatom is a metal cluster composed of plural atoms and is not merely an aggregation of atoms; a metal cluster is stably formed by the aggregation of a magic number of atoms [1–5]. Due to this phenomenon, it has been reported that the cluster structure is difficult to decompose and is stable energetically. Superatoms show the same chemical properties as atoms [6–8]. Superatoms can replace existing substances by exhibiting the atom's chemical properties; the impact of research results on this topic is immeasurable. Such superatoms are known as “artificial elements”. In other words, superatoms are substances that can produce precious metals from inexpensive base metals. Therefore, it is interesting to search for various superatoms and find the corresponding superatoms for all kinds of atoms located in the periodic table. However, many aspects of the electronic states of superatoms are yet to be clarified. The purpose of this study is to investigate a new theoretical route for “modern alchemy”, which is expected to comprise “superatomic material”.

A representative example of a superatom is a metal cluster  $Al_{13}$  with an Al atom at the center of the polyhedron and a framework of 12 Al atoms surrounding the central Al atom. It is a stable regular icosahedron ( $I_h$ ) structure composed of 13 Al atoms, known as the most famous superatom. It has been confirmed experimentally that the chemical properties of the metal cluster  $Al_{13}$  are very similar to those of halogen atoms, such as the Cl and I atoms [9–12]. The fact that the metal cluster  $Al_{13}$  exhibits the same chemical properties as halogen atoms is explained by its electronic configuration.

It is known that electrons are successively occupied by stable atomic orbitals. According to the Pauli exclusion principle, there are no electrons with precisely the same four quantum numbers, and electrons exist in different phase spaces. This difference is also an

essential factor that reveals the properties of various atoms and substances. Atoms contain orbitals such as 1s, 2s, 2p, 3s, 3p, and 3d, and each orbital is occupied by electrons [13]. On the other hand, superatomic orbitals different from atomic orbitals have orbitals such as 1S, 1P, 1D, 2S, 1F, and 2P. Atomic orbitals are described using lowercase letters, while superatomic orbitals are described in uppercase letters. The free electrons in superatoms behave as one unit throughout the cluster; this is called the Jellium model [14].

Here, the reason why the metal cluster  $\text{Al}_{13}$  exhibits properties similar to those of chlorine atoms is explained. The outermost shell orbital of a chlorine (halogen) atom is the 3p orbital, and five electrons occupy the p orbitals ( $p^5$ ).

Therefore, by occupying one more electron, a closed-shell structure is achieved and rendered energetically stable. On the other hand, in the superatom  $\text{Al}_{13}$  metal cluster, there are 13 trivalent Al (III) atoms, and  $3 \times 13 = 39$  valence electrons in total. These 39 valence electrons are occupied in the order of energetically stable superatomic orbitals: 1S, 1P, 1D, 2S, 1F and 2P, respectively. The HOMOs (highest-occupied molecular orbitals) of the  $\text{Al}_{13}$  cluster are the 2P orbitals, and five electrons are occupied in the 2P orbitals ( $P^5$ ). In other words, from the perspective of electron configuration, when the two types of material are compared, the types of electron configuration occupied are identical. The fact that electrons are occupied in each orbital with the same phase (s, p, d, f  $\rightleftharpoons$  S, P, D, F) explains why they have the same chemical properties [15]. Moreover, it has been reported that the superatom  $\text{Al}_{13}$  cluster is used as a single halogen atom [16]. Therefore, it is essential to evaluate materials from the perspective of electron stability. In this study, we attempted to clarify the properties of superatoms by the discrete variational  $X\alpha$  potential molecular orbital calculation method (DV- $X\alpha$  method), which is one of the first principles of calculation. The details of this method are explained in Section 2.

In 2017, a group led by Prof. Yamamoto of the Tokyo Institute of Technology succeeded in synthesizing  $\text{Al}_{13}^-$  in a solution using pyridine core dendrimer (pyDPAG4) [17]. In this vein, there are a large number of methods for synthesizing superatoms. Various metal clusters [18–21] other than  $\text{Al}_{13}$  are synthesized to express different chemical characteristics, depending on the metal cluster. Not only experimental results, but also many theoretical research reports have also been published [22–25]. J. Poater and M. Solà reported that the Jellium model, with its magic numbers, can also be extended to open-shell half-filled systems [26]. One of the methods used to develop the chemical characteristics is a method of constituting a metal cluster not only with one kind of metal atom, but also by combining different metal atoms. With this method, many kinds of superatom are assumed. It is expected that these metal clusters are regarded as building blocks as artificial elements and used for functional materials.

## 2. Materials and Methods

In the analysis of the electronic structure of the six-coordinated octahedral metal complex, we performed the electronic structure calculation based on the DV- $X\alpha$  molecular orbital method. Here, we explain the framework of the calculation method.

The calculating principle of the  $X\alpha$  method is adopted as a special case of a density functional approach based on the Hohenberg–Korn (HK) theorem [27,28]. The HK theorem states that the ground-state energy of a system (assumed to be non-degenerate) is uniquely determined as a function of electron density.

$$\rho(r) = \sum_{k=1}^N |\Psi_k(r)|^2,$$

where  $N$  is the number of the sample points. The  $\Psi_k$  is a one-electron wavefunction, which obeys the Hartree–Fock–Slater equation,

$$H\Psi_k = E_k\Psi_k,$$

Consequently, the one-electron Hamiltonian  $H$  is given by

$$H = -\frac{1}{2}\nabla_i^2 + V(\mathbf{r}) + \int d[b]r' \frac{\rho(r')}{|r - r'|} + \frac{\delta E_{XC}}{\delta \rho}, \quad (1)$$

where  $V(\mathbf{r})$  is the Coulomb potential of the nuclei. In the local density approximation (LDA), the last term of Equation (1) is approximated in the form of  $\delta E_{XC} / \delta \rho = d(\rho \varepsilon_{XC}) / d\rho$ . In the  $X\alpha$  method,  $\varepsilon_{XC}(\rho)$  is the exchange energy of free electron gas multiplied by a constant  $\alpha$ :

$$\varepsilon_{XC}(\rho) = -6\alpha \left[ \frac{3}{4\pi} \rho \right]^{\frac{1}{3}}, \quad (2)$$

Setting  $\alpha = 0.7$  usually makes a good approximation. A self-consistent equation is given from Equations (1) and (2). This one-electron approximation is the self-consistent field method (SCF method) proposed by Hartree in 1928 and includes the Hartree–Fock–Slater method proposed by J. C. Slater [29]. The electronic potential proposed by Slater is called “ $X\alpha$  potential”; the DV- $X\alpha$  method is another name for the Hartree–Fock–Slater method. The DV- $X\alpha$  method was developed by D. E. Ellis (Northwestern University) and Hirohiko Adachi (Kyoto University) [30–34]. The molecular wavefunctions were expressed as linear combinations of atomic orbitals (LCAO) obtained by numerically solving the Hartree–Fock–Slater equations in the atom-like potential derived from the molecular potential. Thus, the atomic orbitals as basic functions are automatically optimized for the molecule. The matrix elements in the secular equation,

$$(H - ES) \times C = 0$$

are derived from the weighted sum of integrand values at sampling points. The overlap charge densities are partitioned into atomic charges by means of Mulliken population analysis [35–38] using the self-consistent charge (SCC) method that is used to approximate the complete self-consistent field. The atomic potentials for generating the basic functions are derived from the spherical average of the molecular charge density around the nuclei, considering the potential tail of the neighboring atoms. The computational details of the method used in the present work have been described elsewhere [39]. The DV- $X\alpha$  method has the advantage of numerically evaluating the electronic state of a substance because the secular equation is solved by the numerical integration. Therefore, accurate calculation results can be obtained for the d- and f-orbitals of the metal ions. Due to the above advantages, the DV- $X\alpha$  method is used.

In this section, the electronic structure of a metal cluster composed of plural atoms is described from the perspective of molecular orbitals. We calculated the electronic structures of the derivatives of the superatom  $\text{Ga}_{13}$  composed of thirteen Ga atoms with three valence electrons per Ga atom, in which the central Ga atom is substituted by another atom (i.e., from  $\text{Ga@Ga}_{12}$  to  $\text{X@Ga}_{12}$ ) in each calculation model. We substituted the central Ga atom with the second, third, and fourth periodic elements of the periodic table ( $\text{X} = \text{Li}, \text{Be}, \text{B}, \text{C}, \text{N}, \text{O}, \text{F}, \text{Ne}, \text{Na}, \text{Mg}, \text{Al}, \text{Si}, \text{P}, \text{S}, \text{Cl}, \text{Ar}, \text{K}, \text{Ca}, \text{Ga}, \text{Ge}, \text{As}, \text{Se}, \text{Br}, \text{and Kr}$ ). The superatom  $\text{Ga}_{13}$  has been confirmed to have similar chemical properties to the iodine atom. The superatom  $\text{Ga}_{13}$  has been widely studied in the same way as the superatom  $\text{Al}_{13}$ . We targeted the superatom  $\text{Ga}_{13}$  as a calculation model.

The absolute coordinates of the calculated cluster model were determined by the reported experimental data based on the bonding distances between two Ga atoms [40]. The  $\text{Ga}_{13}$  cluster has a highly symmetrical regular icosahedron ( $I_h$ ) structure. The superatom  $\text{Ga}_{13}$ , composed of 13 Ga atoms, has an icosahedral cage of 12 Ga atoms around a central Ga atom. It has a bond distance of 2.547 Å from the central Ga atom to the surrounding Ga atoms on the icosahedral cage. The specific details of the structures of  $\text{M@Ga}_{12}$  ( $\text{M} = \text{C}, \text{Si}, \text{Ge}, \text{Sn}, \text{and Pb}$ ) clusters have already been reported in a previous paper [41]. The interatomic distance of 2.547 Å is the most stable bonding distance between the central M atom and a Ga atom on the  $\text{Ga}_{12}$  cage.

The calculations are performed consistently until the difference in orbital populations between the initial and final states of the iteration by means of the DV- $X\alpha$  molecular orbital method is less than 0.0001 electrons. For details of the calculation results, please see the section, Supplementary Materials.

### 3. Results and Discussion

#### 3.1. Wave Functions of Superatomic Orbitals and Hybridization Ratio of Atomic Orbitals in the Superatom $Ga_{13}$

The energy levels of the superatom  $Ga_{13}$  obtained by the first-principle calculation are shown in Figure 1. In the horizontal axis of Figure 1, the serial numbers of the molecular orbitals are plotted. The orbital energy levels of the molecular orbitals are plotted in the vertical axis. Furthermore, the “superatomic orbitals” are also described as “SAOs” below.

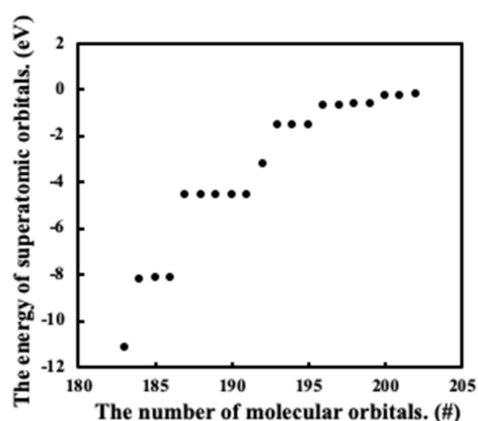


**Figure 1.** Energy levels of superatom  $Ga_{13}$ . These plots are composed of the outer shell electrons from #183 to #202.

The molecular orbitals shown in Figure 1 are the energy levels filled with 39 valence electrons of the superatom  $Ga_{13}$  cluster. The total valence electrons are given by 13 Ga atoms with three valence electrons in each Ga atom ( $39 = 3 \times 13$ ). The orbital energy levels lower than #183 (from #1 to #182) are the inner-shell orbitals of the superatom  $Ga_{13}$ . They correspond to the orbitals that are different from the molecular orbitals filled by the 39 valence electrons. On the other hand, the molecular orbitals from #183 to #202 correspond to the SAOs created by the Jellium model in the  $Ga_{13}$  cluster. It was confirmed that the wave functions of the SAOs are composed of the outermost shell electrons by VESTA (3D wave-function visualization software) [36]. The wave functions of the SAOs are shown in Figure 2.

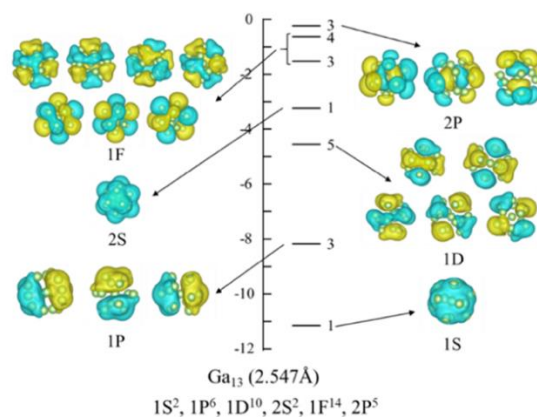


**Figure 2.** Energy levels and the wave functions of the superatomic orbitals of the superatom  $Ga_{13}$  cluster (interatomic Ga–Ga bond distance is 2.547 Å).

The energy levels of the SAOs and the number of degenerated molecular orbitals at each energy level of the superatom  $\text{Ga}_{13}$  are shown in Figure 2. The formation of the SAOs was judged from the VESTA in each wave function. The SAOs corresponded to the 1S, 1P, 1D, 2S, 1F, and 2P orbitals. Furthermore, the 39 valence electrons are occupied in descending order of energy level; the electronic configuration is described as  $1S^2, 1P^6, 1D^{10}, 2S^2, 1F^{14}$ , and  $2P^5$  ( $2 + 6 + 10 + 2 + 14 + 5 = 39$ ). On the other hand, the electronic configuration of the iodine atom ( $Z = 53$ ) is  $[\text{Kr}]^{36}, 4d^{10}, 5s^2$ , and  $5p^5$ . Compared to each outermost orbital, both the  $2P^5$  orbitals ( $\text{Ga}_{13}$ ) and the  $5p^5$  orbitals (iodine atom) acquire another electron to achieve a closed-shell structure. From this fact, it can be understood that the molecular orbitals (=the superatomic orbitals) of the  $\text{Ga}_{13}$  cluster have the same electronic configuration as the atomic orbitals. The superatom  $\text{Ga}_{13}$  has the same “homogeneity” as the iodine atom because it has the same electronic configuration. In Figures 1 and 2, the threefold-degenerated 1F orbitals of the superatom  $\text{Ga}_{13}$  are divided into two groups of threefold (from #193 to #195) and fourfold-degenerated orbitals (from #196 to #199) due to the spin–orbit interaction. The Jellium model is considered to be a perfect sphere. However, the actual  $\text{Al}_{13}$  and  $\text{Ga}_{13}$  are different from perfect spheres because they are polyhedra and icosahedra. Therefore, the symmetry is lowered from spherical symmetry and split into threefold and fourfold.

Next, a Mulliken population analysis was performed to determine which Ga atomic orbitals constitute these SAOs, and the calculation results are shown in Figure 3. In Figure 3, the length of the horizontal axis shows the relative proportions of the atomic orbitals, and the vertical axis shows the serial numbers of the molecular orbitals corresponding to each SAO of the  $\text{Ga}_{13}$  cluster. For example, molecular orbital #183 corresponds to the 1S superatomic orbital. The 1S superatomic orbital can be produced as the summation of atomic orbitals such as the outer (cage) Ga 4s orbitals (about 57.5%), the 4p orbitals (about 14.9%), and the central Ga 4s orbitals (about 24%). The 1S (#183) and 2S (#192) orbitals of the SAOs contain the 4s orbitals of the central Ga atom (orange). The 1P (from #184 to #186) and 2P (from #200 to #202) orbitals contain the 4p orbitals of the central Ga atom (purple). The symmetry of the atomic orbitals of the central Ga atom (4s or 4p orbitals) is expected. Therefore, it is closely related to the symmetry of the SAOs. It is possible to change the properties of the entire superatom significantly, depending on the number of electrons in the central metal and the orbitals of the outermost shell.

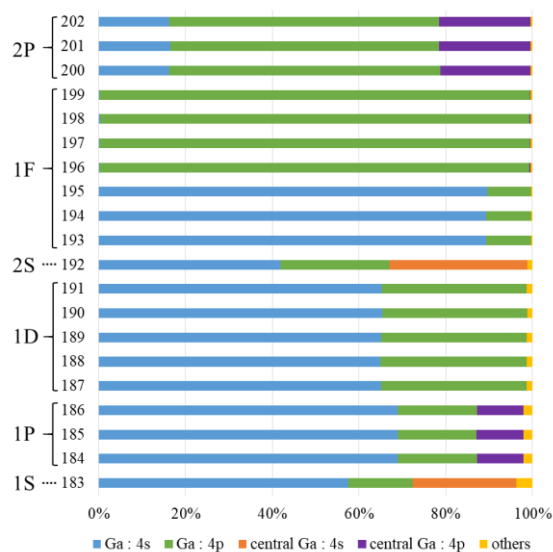


**Figure 3.** Ratio of atomic orbitals in order to create the superatomic orbitals of the  $\text{Ga}_{13}$  cluster (interatomic Ga–Ga bond distance is 2.547 Å) by means of the Mulliken population analysis.



### 3.2. The Effects of the Atom Substituted for the Central Atom in the $\text{Ga}_{13}$ Cluster ( $\text{X@Ga}_{12}$ )

As described in Section 3.1, it was revealed that the symmetry of the central Ga atomic orbitals dramatically contributes to the symmetry of the superatomic orbitals. Next, we considered the effect of substituting the central Ga atom in  $\text{Ga}_{13}$ . By confirming the molecular orbitals in the superatom-like  $\text{X@Ga}_{12}$  cluster, we confirmed whether some orbitals similar to superatomic orbitals were shown. This was because it was expected that the group of atoms in the superatom-like  $\text{X@Ga}_{12}$  cluster would not necessarily have the characteristics of the superatom. The similar superatomic orbitals are named “superatom-like orbitals”, described as “SALOs” below. Superatomic-like orbitals (=SALOs) are not to be confused with superatomic orbitals (=SAOs), as described in Section 3.1.

Therefore, we considered the effect of substituting the central Ga atom in  $\text{Ga}_{13}$ , that is, the superatom-like  $\text{X@Ga}_{12}$  cluster models were set as the calculation models in Figure 4. The substituted central atom was selected as the second, third, or fourth periodic element in the periodic table. ( $\text{X} = \text{Li, Be, B, C, N, O, F, Ne, Na, Mg, Al, Si, P, S, Cl, Ar, K, Ca, Ga, Ge, As, Se, Br, and Kr}$ ). In addition to substituting another atom for the central Ga atom, the bond distance between the atoms within the cluster size was also changed. The cluster models were prepared for two kinds of bond distance (the interatomic X–Ga bond distance is 2.547 or 2.944 Å). The effects of the two parameters, the type of central atom, and the interatomic bond distance in the cluster model on the generation of SALOs were examined. We also aimed to obtain the chemical properties of the superatoms. The reason why the bond distance between the two Ga atoms was set at 2.944 Å is that the longest bond distance was confirmed in the  $\text{M@Ga}_{12}$  ( $\text{M} = \text{C, Si, Ge, Sn and Pb}$ ) results. The effects of the two parameters, the type of central atom, and the interatomic bond distance in the cluster model, and how these would relate to the generation of the SALOs, were examined.

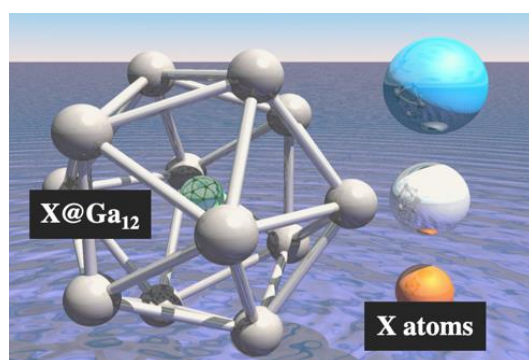


**Figure 4.** Cluster models  $\text{X@Ga}_{12}$  ( $\text{X} = \text{Li} \sim \text{Kr}$ ) substituted for a central atom in the icosahedral  $\text{Ga}_{12}$  cage.

The changes in energy levels and the effects of the two parameters were examined. Each two parameters are a type of central atom, and the interatomic bond distance in the cluster model, in the generation of the SALOs (1D, 1F, 2S, and 2P orbitals). The results of the energy levels of these cluster models are summarized in Figures 5 and 6 for the X–Ga interatomic bond distances (2.547 Å, 2.944 Å). Here, the respective SALOs are plotted with the atomic species substituted as the central atom (X) on the horizontal axis and the orbital energy of the superatom-like  $\text{X@Ga}_{12}$  cluster on the vertical axis. The effects of the two parameters, the type of central atom, and the interatomic bond distance in the cluster model on the generation of the SALOs were examined.

From these results, it was confirmed that the energy levels of SALOs such as the 2S and 2P change periodically when substituting the central atom. This reflects the periodicity in the periodic table of the substituted atom despite the fact that the bond distance between two Ga atoms also changed. In Figures 5 and 6, only the 1D, 2S, 1F, and 2P SLAOs are shown. This is because the energy levels of the inner 1S and 1P SLAOs were much lower than those of other SALOs, such as the 2S and 1F SLAOs. Even if the central atom is substituted, the orbital energy of 1S or 1P SLAOs does not change significantly. Furthermore, as the atomic

number of the central atom increases, the number of valence electrons also increases. There are some energy gaps at these points, as shown in Figures 5 and 6.

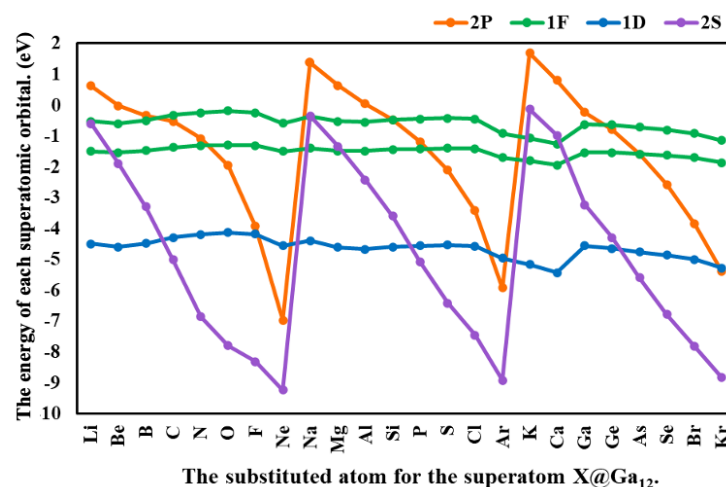


**Figure 5.** Energy levels of the 2P (purple), 1F (green), 1D (blue), and 2S (orange) superatomic-like orbitals, respectively, in the  $X@Ga_{12}$  cluster (interatomic X–Ga bond distance is 2.547 Å).

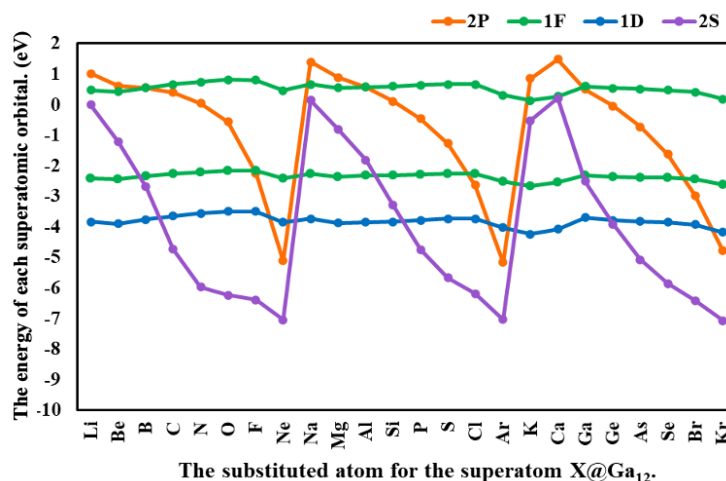


**Figure 6.** Energy levels of the 2P (purple), 1F (green), 1D (blue), and 2S (orange) superatomic-like orbital, respectively, in the  $X@Ga_{12}$  cluster (interatomic X–Ga bond distance is 2.944 Å).

When substituting the central atom X in the cluster model of the superatom-like  $X@Ga_{12}$  with various atoms, the energy levels of the 1D and 1F SLAOs hardly change. On the other hand, the “periodicity” reflecting the substituted atom can be confirmed for the 2S and 2P SLAOs. For example, when the first-group element ( $X = Li, Na, K$ ), an alkali metal, is substituted, the 2P SLAOs have higher energy than the 1F orbitals, as shown in Figure 5. Moreover, the 2S SLAOs are located between the two split 1F orbitals. However, the atomic number of the substituted central atom increases in order from the alkali metal, and the energy levels of both the 2S and the 2P SLAO decrease. Finally, when the substituted central atom is replaced by the noble gas elements ( $X = Ne, Ar, Kr$ ), the energy level decreases the most. The energy of the 2S and 2P SLAOs is much lower than that of the 1D SLAO. This is because the noble gas elements are more stable in single atoms than in other atoms. When they become the central atoms in the cluster model of the superatom-like  $X@Ga_{12}$ , the central noble gas atoms do not interact with the electrons of the atoms constituting the surrounding  $Ga_{12}$  cages, and the electron repulsion is suppressed.

The central atom X of the superatom-like  $X@Ga_{12}$  ( $X = Li \sim Kr$ ) is the s or p block atom in the typical periodic table. The outermost shell orbitals are the 2s (or 3s, or 4s) or 2p (or

3p, or 4p) atomic orbitals. By substituting these atoms into the central atom in the  $\text{Ga}_{12}$  cage, the electron repulsion reflecting the symmetry of the atomic orbital of the central atom is expected to affect the electron disruption in the superatom  $\text{Ga}_{13}$  cluster. When we consider the symmetry between the atomic orbitals and superatomic-like orbitals, the s, p, d, and f atomic orbitals have the same symmetry as the S, P, D, and F SALOs, respectively. These orbitals are considered to have a strong, symmetrical correlation. Both the s and p atomic orbitals have a large shielding effect, suggesting that the s and p atomic orbitals interact strongly with both the S and P SALOs. Therefore, in Figures 5 and 6, the energy change in the 2S and 2P SALOs has a large periodicity, reflecting the periodicity of the s and p atomic orbitals in the central atom. On the other hand, the 1D and 1F SALOs receive a slight shielding effect from the central atom because of the s or p block atoms. In other words, the electrons in the D and F SALOs are less affected by the atomic orbitals of the central metal than the electrons in the S and P SALOs.

As in the substitution of the central atom, the energy level changes of the “periodicity” SALOs were confirmed when the interatomic bond distance between the central atom X and a surrounding Ga atom was changed. The most significant change was in the energy levels of two split 1F SALOs. The energy difference was larger at 2.547 Å compared to at 2.944 Å. For example, when an Al atom is substituted as the central atom ( $\text{Al@Ga}_{12}$ ), the electron configuration is  $1\text{S}^2, 1\text{P}^6, 1\text{D}^{10}, 2\text{S}^2, 1\text{F}^{14}$ , and  $2\text{P}^5$ , with no splitting of 1F orbitals at the 2.547 Å interatomic Al–Ga bond distance. However, at the 2.944 Å bond distance, the 2S SALOs locate between the split three- and four-fold 1F SALOs. As a result, the electron configuration changes as follows:  $1\text{S}^2, 1\text{P}^6, 1\text{D}^{10}, 1\text{F}^6, 2\text{S}^2, 1\text{F}^8$ , and  $2\text{P}^5$ .

From these results, it was inferred that the energy level of the 1D or 1F SALOs was controlled and caused the SCO (spin crossover) observed in the metal complex. There is a sufficient likelihood of controlling the SALOs by applying the bond distance changes and the distortion of the structure with external energy from the heat, light, light, and magnetic fields. By controlling the bond distances and symmetrical distortions of the SALOs, it is possible to design and synthesize the novel superatoms with switchable magnetic properties.

Next, we examined whether the hybridizations among the SALOs could be expressed in superatoms and shown in the hybridized orbital behavior in an atom. First, the arsenic atom substituted in the central atom  $\text{As@Ga}_{12}$  is described. In this case, the energy levels of the SALOs overlap with the lower energy of the 2P and the split 1F SALOs. There are six hybridized SALOs, named  $\text{F}^3\text{P}^3$  orbitals, consisting of three 2P and three 1F SALOs. The wave functions of the hybridized  $\text{F}^3\text{P}^3$  SALOs are shown in Figure 7. The ratio of atomic orbitals whose atoms constitute their SALOs obtained through the Mulliken population analysis is shown in Figure 8.

In Figure 8, the 4p orbitals of the arsenic atom (purple) are dispersed in the six SALOs from #193 to #198 in the results of the Mulliken population analysis. Therefore, the 1F and 2P SALOs of the superatom-like  $\text{As@Ga}_{12}$  (the interatomic As–Ga bond distance is 2.547 Å) can form hybridized  $\text{F}^3\text{P}^3$  SALOs. The energy levels of the SALOs are close to each other. Therefore, the interaction between the hybridized SALOs becomes strong. When the central metal was substituted with an atom other than the arsenic atom, similar hybridized SALOs were confirmed not only in the 1F and 2P hybridized SALOs, but also in the 2S and 1F hybridized SALOs. It was understood that this concept of hybridized SALOs was necessary to the interpretation of the SALOs. It was also discovered that the electronic structure of the superatom can be controlled by changing the bond distances, the structural distortions, and the central atom of the superatom  $\text{Ga}_{12}$  cage.



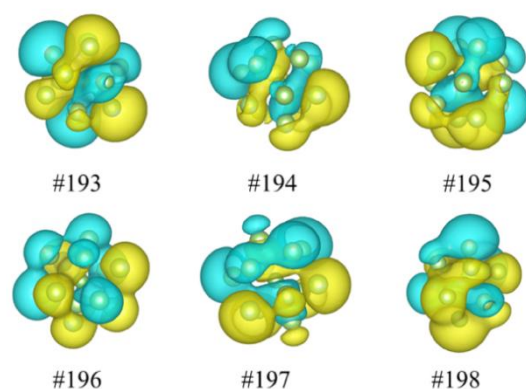


**Figure 7.** Wave functions of the hybridized  $F^3P^3$  superatomic-like orbitals of superatom-like  $As@Ga_{12}$  cluster (the interatomic As–Ga bond distance is 2.547 Å). The superatomic-like wave functions are described in #193, #194, #195, #196, #197, and #198 superatomic-like orbitals, respectively.

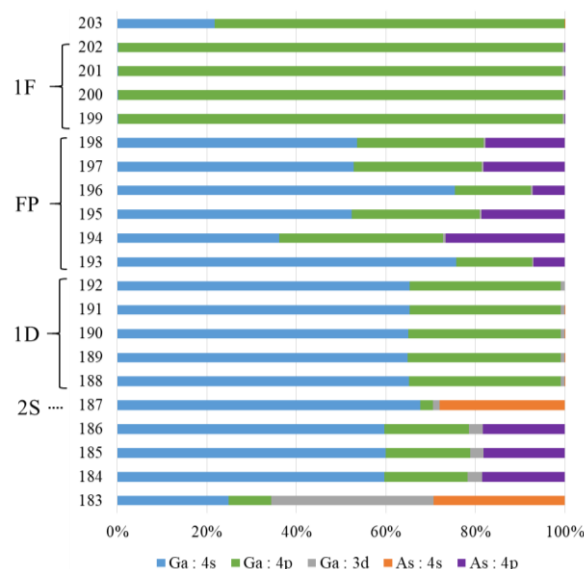


**Figure 8.** Ratio of atomic orbitals in order to create the superatomic-like orbitals of the  $As@Ga_{12}$  cluster (interatomic As–Ga bond distance is 2.547 Å) by means of the Mulliken population analysis. The term “FP” from #193 to #198 denotes the hybridized  $F^3P^3$  superatomic-like orbitals.

### 3.3. The Limit of the Conditions for Applying the Jellium Model

In Section 3.2, it was shown that the molecular orbital calculations of the superatom-like  $X@Ga_{12}$  cluster have superatomic-like orbitals. In Section 3.3, it is explained that the change in the size of the superatom-like  $X@Ga_{12}$  cluster relates to the collapse of the Jellium state and that the molecular orbitals are simply composed of LCAOs. The boundary conditions between the superatom-like orbitals (Jellium model) and LCAOs are reported in four cluster models.

Among the 48 kinds of superatom-like  $X@Ga_{12}$  cluster model, four superatom-like clusters (whose interatomic Ga–Ga bond distance is 2.547 Å),  $Ga_{13}$ ,  $Be@Ga_{12}$  (Be–Ga is 2.547 Å),  $B@Ga_{12}$  (B–Ga is 2.547 Å), and  $Al@Ga_{12}$  (Al–Ga is 2.547 Å), were found to have an electron configuration close to the perfect spherical symmetry according to the ideal Jellium model. In these four spherically symmetrical Jellium models, if the bond distance between the central atom X and a surrounding Ga atom is extended (or shrunk), more than necessary, the Jellium model is expected to collapse at a certain distance. Therefore, in each of the four models, it was determined whether the Jellium model was “constituted” or “not constituted”, which means whether the condition of the LCAO (Linear combination of

atomic orbitals) can be satisfied or not by expanding (or shortening) the bond distance, as shown in Figure 9.

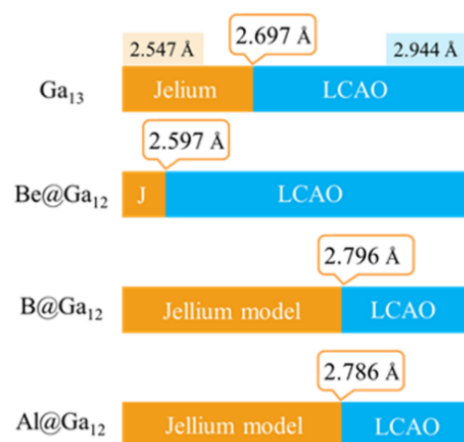


**Figure 9.** Boundary of the condition of the interatomic X–Ga bonding distance for Jellium model constitution of the clusters Ga<sub>13</sub>, Be@Ga<sub>12</sub>, B@Ga<sub>12</sub>, and Al@Ga<sub>12</sub>, respectively (interatomic Ga–Ga bond distance is 2.547 Å).

From the results shown in Figure 9, it can be seen that Ga<sub>13</sub>, B@Ga<sub>12</sub>, and Al@Ga<sub>12</sub> do not collapse the Jellium model even if the bond distances between the central atom X and the Ga atom are extended from 2.547 Å to 2.697 Å, 2.796 Å, and 2.786 Å, respectively. However, in the case of Be@Ga<sub>12</sub>, an extension of only about 0.05 Å (from 2.547 to 2.597 Å) resulted in the collapse of the Jellium model. This was because the elements of Ga, B, and Al were all “group 3” atoms on the periodic table with three valence electrons. The typical superatom Al<sub>13</sub> is composed of 39 valence electrons and 13 atoms, with three valence electrons per atom. The possibility of the magic number of total valence electrons that can stably exist is anticipated. In the case of the bond distance near the boundary between the condition of the Jellium model and the LCAO model, it was confirmed that hybridized SALOs were formed when the aforementioned SALOs were substituted by other atoms.

It was found that the appropriate cage size for creating the Jellium model differs greatly depending on the central metal, even if the superatom-like X@Ga<sub>12</sub> has the same Ga<sub>12</sub> cage. These calculation results also indicated that the conditions for creating superatoms are quite delicate. The electronic structure can be greatly changed not only by the symmetry of the atomic orbitals of the central atom but also by slight changes, such as the interatomic bond distance between the X and Ga atoms and the distortion of the SALOs.

#### 4. Conclusions

The effect of substituting various atoms for the central atom in Ga<sub>13</sub> was considered from the molecular orbital calculation in the superatom-like X@Ga<sub>12</sub>. As a result, two characteristics of the superatomic-like orbitals (=LCAOs) were determined.

The first characteristic is periodicity. By substituting the central atom with various atoms, the “periodicity” of the energy level was confirmed in the 2S and 2P SLAOs. This was attributed to the shielding effect of the central atom and the symmetry of the atomic orbitals. It was concluded that the outermost shell orbitals of the central atom were the 2s or 2p atomic orbitals, which produce electronic repulsion along with the symmetry of the atomic orbitals with the Ga<sub>12</sub> cage. The S and P SLAOs correspond to the symmetry of the central atomic orbitals from the SALOs by interacting with the electrons in the Jellium model.

The second characteristic is the alternation of the Jellium state by substituting the central X atom in the superatom-like X@Ga<sub>12</sub> clusters. Among the 48 kinds of superatom-like X@Ga<sub>12</sub> cluster, some superatoms have an electronic configuration according to the Jellium model, such as the superatoms Ga<sub>13</sub>, Be@Ga<sub>12</sub>, B@Ga<sub>12</sub>, and Al@Ga<sub>12</sub> (whose interatomic X–Ga bond distance is 2.547 Å). By extending the bond distances between the

central atom X and the Ga atom by about 0.14 Å ( $\text{Ga}_{13}$ ), 0.05 Å ( $\text{Be@Ga}_{12}$ ), 0.249 Å ( $\text{B@Ga}_{12}$ ), and 0.239 Å ( $\text{Al@Ga}_{12}$ ), the Jellium model was collapsed, and the LCAO was formed. The results show that SALOs can be controlled by changing the bond distance by using external energy such as heat, light, or a magnetic field, and by the spin cross-over phenomenon. Controlling the superatom effectively changes the bond distance or symmetry distortion in the superatom. Superatom synthesis with the physical and chemical properties of specific atoms can be achieved. In addition, we believe that it is possible to predict chemical and physical properties in advance and provide meaningful results concerning superatoms.

**Supplementary Materials:** The following supporting information can be downloaded at: <https://www.mdpi.com/article/10.3390/cryst12040543/s1>, Figures S1–S48. The list of calculation results of the Mulliken Population Analysis in each superatomic-like  $\text{X@Ga}_{12}$  cluster model used for the one-electron calculation (DV- $\text{X}\alpha$  molecular orbital method).

**Author Contributions:** T.N. and T.T. performed the research tasks, such as the theoretical calculation. T.T., and T.I. designed this project. G.S. gave us a new interpretation and meaningful data (in Figures 2 and 7). T.N., T.T. and T.I., contributed to the discussion of the results. T.N. and T.I. revised the manuscript. All authors have read and agreed to the published version of the manuscript.

**Funding:** T.I. is supported by JSPS KAKENHI grant 20H00362.

**Institutional Review Board Statement:** Not applicable.

**Informed Consent Statement:** Not applicable.

**Data Availability Statement:** Not applicable.

**Acknowledgments:** The authors express their thanks to F. Izumi (National Institute for Materials Science, Japan) and K. Momma (National Museum of Nature and Science, Tokyo) for permission to use a 3D visualization program, “VESTA”. The authors thank H. Adachi (Kyoto Univ.) for permission to use a computational program. The article (DOI 10.1002/qua.22044) published by T.I. is the important reference paper in this article.

**Conflicts of Interest:** The authors declare no conflict of interest.

## References

- De Heer, W.A. The physics of simple metal clusters: Experimental aspects and simple models. *Rev. Mod. Phys.* **1993**, *65*, 611. [CrossRef]
- Leuchtner, R.E.; Harms, A.C.; Castleman, A.W., Jr. Thermal metal cluster anion reactions: Behavior of aluminum clusters with oxygen. *J. Chem. Phys.* **1989**, *91*, 2753–2754. [CrossRef]
- Luo, Z.; Grover, C.J.; Reber, A.C.; Khanna, S.N.; Castleman, A.W., Jr. Probing the magic numbers of aluminum–magnesium cluster anions and their reactivity toward oxygen. *J. Am. Chem. Soc.* **2013**, *135*, 4307–4313. [CrossRef] [PubMed]
- Brack, M. The physics of simple metal clusters: Self-consistent Jellium model and semiclassical approaches. *Rev. Mod. Phys.* **1993**, *65*, 677. [CrossRef]
- Knight, W.D.; Clemenger, K.; de Heer, W.A.; Saunders, W.A.; Chou, M.Y.; Cohen, M.L. Electronic shell structure and abundances of sodium clusters. *Phys. Rev. Lett.* **1984**, *52*, 2141. [CrossRef]
- Luo, Z.; Castleman, A.W. Special and general superatoms. *Acc. Chem. Res.* **2014**, *47*, 2931–2940. [CrossRef]
- Bergeron, D.E.; Roach, P.J.; Castleman, A.W.; Jones, N.O.; Khanna, S.N. Al cluster superatoms as halogens in polyhalides and as alkaline earths in iodide salts. *Science* **2005**, *307*, 231–235. [CrossRef]
- Bergeron, D.E.; Castleman, A.W.; Morisato, T.; Khanna, S.N. Formation of  $\text{Al}_{13}\text{I}^-$ : Evidence for the superhalogen character of  $\text{Al}_{13}$ . *Science* **2004**, *304*, 84–87. [CrossRef]
- Bergeron, D.E.; Castleman, A.W., Jr.; Morisato, T.; Khanna, S.N. Formation and properties of halogenated aluminum clusters. *J. Chem. Phys.* **2004**, *121*, 10456–10466. [CrossRef]
- Schnöckel, H.; Köhnlein, H. Synthesis and structure of metalloid aluminum clusters—Intermediates on the way to the elements. *Polyhedron* **2002**, *21*, 489–501. [CrossRef]
- Luo, Z.; Berkdemir, C.; Smith, J.C.; Castleman, A.W., Jr. Cluster reaction of  $[\text{Ag}_8]^-/[\text{Cu}_8]^-$  with chlorine: Evidence for the harpoon mechanism? *Chem. Phys. Lett.* **2013**, *582*, 24–30. [CrossRef]
- Zhang, X.; Wang, Y.; Wang, H.; Lim, A.; Gantefoer, G.; Bowen, K.H.; Reveles, J.U.; Khanna, S.N. On the existence of designer magnetic superatoms. *Acc. Chem. Res.* **2013**, *135*, 4856–4861. [CrossRef] [PubMed]

13. Reber, A.C.; Khanna, S.N. Superatoms: Electronic and geometric effects on reactivity. *Acc. Chem. Res.* **2017**, *50*, 255–263. [[CrossRef](#)] [[PubMed](#)]
14. Hughes, R.I. Theoretical practice: The Bohm-Pines quartet. *Perspect. Sci.* **2006**, *14*, 457–524. [[CrossRef](#)]
15. Khanna, S.N.; Jena, P. Atomic clusters: Building blocks for a class of solids. *Phys. Rev. B* **1995**, *51*, 13705. [[CrossRef](#)]
16. Castleman, A.W., Jr.; Khanna, S.N. Clusters, superatoms, and building blocks of new materials. *J. Phys. Chem. C* **2009**, *113*, 2664–2675. [[CrossRef](#)]
17. Kambe, T.; Haruta, N.; Imaoka, T.; Yamamoto, K. Solution-phase synthesis of  $\text{Al}_{13}^-$  using a dendrimer template. *Nat. Commun.* **2017**, *8*, 1–7. [[CrossRef](#)]
18. Narouz, M.R.; Takano, S.; Lummis, P.A.; Levchenko, T.I.; Nazemi, A.; Kaappa, S.; Malola, S.; Yousefalizadeh, G.; Calhoun, L.A.; Stampelcoskie, K.G.; et al. Robust, highly luminescent  $\text{Au}_{13}$  superatoms protected by N-heterocyclic carbenes. *J. Am. Chem. Soc.* **2019**, *141*, 14997–15002. [[CrossRef](#)]
19. Zhu, M.; Aikens, C.M.; Hendrich, M.P.; Gupta, R.; Qian, H.; Schatz, G.C.; Jin, R. Reversible switching of magnetism in thiolate-protected  $\text{Au}_{25}$  superatoms. *J. Am. Chem. Soc.* **2009**, *131*, 2490–2492. [[CrossRef](#)]
20. Negishi, Y.; Kurashige, W.; Kobayashi, Y.; Yamazoe, S.; Kojima, N.; Seto, M.; Tsukuda, T. Formation of a  $\text{Pd@Au}_{12}$  superatomic core in  $\text{Au}_{24}\text{Pd}_1(\text{SC}_{12}\text{H}_{25})_{18}$  probed by  $^{197}\text{Au}$  Mossbauer and Pd K-Edge EXAFS spectroscopy. *J. Phys. Chem. Lett.* **2013**, *4*, 3579–3583. [[CrossRef](#)]
21. Chen, J.; Yang, H.; Wang, J.; Cheng, S.B. Revealing the effect of the oriented external electronic field on the superatom-polymeric  $\text{Zr}_3\text{O}_3$  cluster: Superhalogen modulation and spectroscopic characteristics. *Spectrochim. Acta A Mol. Biomol. Spectrosc.* **2020**, *237*, 118400. [[CrossRef](#)]
22. Reber, A.C.; Khanna, S.N.; Castleman, A.W. Superatom compounds, clusters, and assemblies: Ultra alkali motifs and architectures. *J. Am. Chem. Soc.* **2007**, *129*, 10189–10194. [[CrossRef](#)]
23. Chattaraj, P.K.; Giri, S. Stability, reactivity, and aromaticity of compounds of a multivalent superatom. *J. Phys. Chem. A* **2007**, *111*, 11116–11121. [[CrossRef](#)] [[PubMed](#)]
24. Jena, P.; Khanna, S.N.; Rao, B.K. Designing clusters as superelements. *Surf. Rev. Lett.* **1996**, *3*, 993–999. [[CrossRef](#)]
25. Jena, P. Beyond the periodic table of elements: The role of superatoms. *J. Phys. Chem. Lett.* **2013**, *4*, 1432–1442. [[CrossRef](#)]
26. Poater, J.; Solà, M. Open-shell jellium aromaticity in metal clusters. *Chem. Commun.* **2019**, *55*, 5559–5562. [[CrossRef](#)] [[PubMed](#)]
27. Hohenberg, P.; Kohn, W. Inhomogeneous Electron Gas. *Phys. Rev.* **1964**, *136*, B864. [[CrossRef](#)]
28. Kohn, W.; Sham, L.J. Self-Consistent Equations Including Exchange and Correlation Effects. *Phys. Rev.* **1965**, *140*, A1133. [[CrossRef](#)]
29. Slater, J.C. A simplification of the Hartree-Fock method. *Phys. Rev.* **1951**, *81*, 385. [[CrossRef](#)]
30. Adachi, H.; Tsukuda, M.; Satoko, C. Discrete variational  $X\alpha$  cluster calculations. I. Application to metal clusters. *J. Phys. Soc. Jpn.* **1978**, *45*, 875–883. [[CrossRef](#)]
31. Satoko, C.; Tsukada, M.; Adachi, H. Discrete variational  $X\alpha$  cluster calculations. II. Application to the surface electronic structure of  $\text{MgO}$ . *J. Phys. Soc. Jpn.* **1978**, *45*, 1333–1340. [[CrossRef](#)]
32. Adachi, H.; Shiokawa, S.; Tsukada, M.; Satoko, C.; Sugano, S. Discrete variational  $X\alpha$  cluster calculations. III. Application to transition metal complexes. *J. Phys. Soc. Jpn.* **1979**, *47*, 1528–1537. [[CrossRef](#)]
33. Adachi, H.; Taniguchi, K. Discrete variational  $X\alpha$  cluster calculations. IV. Application to X-ray emission study. *J. Phys. Soc. Jpn.* **1980**, *49*, 1944–1953. [[CrossRef](#)]
34. Adachi, H.; Mukoyama, T.; Kawai, J. (Eds.) *Hartree-Fock-Slater Method for Materials Science: The DV-X Alpha Method for Design and Characterization of Materials*; Springer Science & Business Media: Berlin/Heidelberg, Germany; New York, NY, USA, 2006; Volume 84, ISBN 978-3-540-31297-0.
35. Mulliken, R.S. Electronic Population Analysis on LCAO–MO Molecular Wave Functions. I. *J. Chem. Phys.* **1955**, *23*, 1833. [[CrossRef](#)]
36. Mulliken, R.S. Electronic Population Analysis on LCAO–MO Molecular Wave Functions. II. Overlap Populations, Bond Orders, and Covalent Bond Energies. *J. Chem. Phys.* **1955**, *23*, 1841. [[CrossRef](#)]
37. Mulliken, R.S. Electronic Population Analysis on LCAO–MO Molecular Wave Functions. III. Effects of Hybridization on Overlap and Gross AO Populations. *J. Chem. Phys.* **1955**, *23*, 2338. [[CrossRef](#)]
38. Mulliken, R.S. Electronic Population Analysis on LCAO–MO Molecular Wave Functions. IV. Bonding and Antibonding in LCAO and Valence-Bond Theories. *J. Chem. Phys.* **1955**, *23*, 2343. [[CrossRef](#)]
39. Ishii, T.; Tsuboi, S.; Sakane, G.; Yamashita, M.; Breedlove, B.K. Universal spectrochemical series of six-coordinate octahedral metal complexes for modifying the ligand field splitting. *Dalton Trans.* **2009**, *4*, 680–687. [[CrossRef](#)]
40. Yuan, G.; Lu, P.; Han, L.; Yu, Z.; Shen, Y.; Zhao, L.; Liu, Y. Structural and electronic properties of neutral clusters  $\text{Ga}_{12}\text{X}$  ( $\text{X} = \text{C}, \text{Si}, \text{Ge}, \text{Sn}, \text{and Pb}$ ) and their anions from first principles. *Phys. B Condens.* **2011**, *406*, 3498–3501. [[CrossRef](#)]
41. Momma, K.; Izumi, F. VESTA: A three-dimensional visualization system for electronic and structural analysis. *J. Appl. Crystallogr.* **2008**, *41*, 653–658. [[CrossRef](#)]